First-order homogeneous electron gas model of semiconductors at finite temperatures

T. L. Li
Department of Applied Physics, National Chia-Yi University, 300 Hsueh-Fu Road, Chiayi 600, Taiwan
(Received 8 March 2001; revised manuscript received 20 February 2002; published 8 May 2002)

The homogeneous electron gas model extensively used in semiconductor physics is extended, leading to the first-order homogeneous electron gas model. The model explicitly accounts for the gradient of potential energy to the first order and is applicable to semiconductors at finite temperatures. With this model, the density of states and the carrier density can be calculated by analytic formulas without having to solve the Schrödinger equation.

DOI: 10.1103/PhysRevB.65.193203 PACS number(s): 71.22.+i, 03.65.−w

I. INTRODUCTION

The homogeneous electron gas (HEG) model of solid-state theory[1] has been extensively utilized in standard semiconductor textbooks.[2,3] In the HEG theory, the electrons are treated as independent particles with a constant potential energy. Since the potential energy is assumed to be independent of the position, all orders of position derivatives of the potential energy identically vanish but the zeroth order. The potential energy operator thus commutes with the kinetic energy operator.[4] Hence, the HEG can be considered as a zeroth-order theory.

Phenomenologically, the potential energy becomes position dependent when an electric field[5–9] or a compositional variation[10–13] or a doping gradient[14] is present and introduces band-bending in semiconductors. Under such circumstances, the potential energy operator and the kinetic energy operator no longer commute,[4] and, rigorously speaking, the zeroth-order HEG is no longer valid, either.

Furthermore, tunneling tails of wave functions into the band edge are known to introduce nonvanishing density of states to the forbidden band gap at the presence of band bending.[5,14] This tunneling effect cannot be modeled by the HEG theory because of its complete negligence of the potential gradient.

In the literature, the symmetrized Hamiltonian was used to account for the position dependence of the electron potential energy to first order;[15,16] the nonlocal density of state was employed to facilitate finite-temperature formulation.[17,18]

In this article, the techniques developed in the symmetrized Hamiltonian[15,16] and the nonlocal density of states[17,18] are combined and utilized to modify the HEG theory, leading to the first-order homogeneous electron gas (FOHEG) model. The FOHEG model explicitly includes the gradient of the potential energy to first order and is applicable to semiconductors at finite temperatures. With this approximation, the density of states and the carrier density can be computed by compact analytic formulas without having to explicitly solve the Schrödinger equation.

II. FIRST-ORDER HOMOGENEOUS ELECTRON GAS THEORY

In the theory of homogeneous electron gas, the carrier concentration of a quantized system is usually calculated by solving the Schrödinger equation for the normalized wave function $\varphi_i(\vec{r})$ with eigenenergy ε_i and, then, summing over all of the squared moduli of the wave functions weighted by the Fermi-Dirac distribution.[1] Alternatively, the carrier density may be calculated by integrating over energy the product of the density of states (DOS) and the Fermi-Dirac distribution,[17,18]

$$n(\vec{r})=2\sum_i |\varphi_i(\vec{r})|^2 f(\varepsilon_i)=\int d\varepsilon D(\vec{r},\varepsilon)f(\varepsilon), \tag{1}$$

where $f(\varepsilon)=1/[1+e^{\beta(\varepsilon-\varepsilon_F)}]$ is the Fermi-Dirac distribution with Fermi level ε_F and $\beta=1/kT$, and the DOS is obtained from the nonlocal density of states (NLDS),

$$D(\vec{r},\vec{r}',\varepsilon)=2\sum_i \delta(\varepsilon-\varepsilon_i)\varphi_i^*(\vec{r}')\varphi_i(\vec{r}), \tag{2}$$

by letting $\vec{r}'$ approach $\vec{r}$. The factor of 2 is to account for the electron spin. If the eigenenergy ε_i is replaced by a symmetrized Hamiltonian, $\frac{1}{2}[\hat{H}(\vec{r})+\hat{H}^\dagger(\vec{r}')]$, as in Refs. 15 and 16, then the algebraic property $D(\vec{r},\vec{r}',\varepsilon)^*=D(\vec{r}',\vec{r},\varepsilon)$ is preserved, and the reality of the DOS may be ensured in the subsequent approximation.

Invoking the integral representation of a δ function and following the treatments in Refs. 15, 16, and 19–21, the exact, but unsolvable, NLDS can be obtained. By retaining only terms with a first-order derivative of the potential energy, an approximate expression may be obtained,

$$D(\vec{r},\varepsilon)\approx 2\int\frac{d\omega}{2\pi}\int\frac{d^d\vec{p}}{(2\pi\hbar)^d}\times\exp\left[i\omega\left(\varepsilon-\frac{\vec{p}^2}{2m}-V(\vec{r})\right)-\frac{i\hbar^2\omega^3}{24m}(\nabla V)^2\right], \tag{3}$$

where d is the dimensionality of the physical system. This approximation only retains the first-order derivative of the potential energy. Hence, it is called the first-order homogeneous electron gas approximation in this work.

By using mathematical techniques in Refs. 22–24, the above integral may be performed, and the DOS is obtained in a rather compact form

 ©2002 The American Physical Society

$$D(\vec{r},\varepsilon)=\frac{2}{\Gamma(d/2)}\left(\frac{m}{2\pi\hbar^2}\right)^{d/2}b^{d/2-1}\int_{-\bar{\varepsilon}}^{\infty}dt\times\mathrm{Ai}(t)(t+\bar{\varepsilon})^{d/2-1},\tag{4}$$

where $b^3=\hbar^2|\nabla V|^2/8m$, and $\bar{\varepsilon}=(\varepsilon-V)/b$. Ai and Γ are Airy and gamma functions, respectively. At the flat-band limit $\nabla V\rightarrow 0$, the DOS becomes

$$D(\vec{r},\varepsilon)\rightarrow\frac{2}{\Gamma(d/2)}\left(\frac{m}{2\pi\hbar^2}\right)^{d/2}(\varepsilon-V)^{d/2-1}\theta(\varepsilon-V),\tag{5}$$

which is the DOS of the homogeneous electron gas model of semiconductors.[2,3]

The carrier density of a quantized system follows from Eqs. (1) and (4) by interchanging the order of the double integral,

$$n(\vec{r})=2\left(\frac{m}{2\pi\hbar^2\beta}\right)^{d/2}\int_{-\infty}^{\infty}dt\,\mathrm{Ai}(t)\mathcal{F}_{d/2-1}[\beta(bt+\varepsilon_F-V)],\tag{6}$$

where

$$\mathcal{F}_j(x)=\frac{1}{\Gamma(j+1)}\int_0^{\infty}dt\frac{t^j}{1+e^{t-x}}$$

is the Fermi-Dirac integral of order j and argument x.[25]

The relations of the FOHEG carrier density in Eq. (6) to other theories will be illustrated in the rest of this section.

First of all, a comparison between the NLDS in Eq. (2) of this work and the density matrix of Ref. 15 is made. When changing to a consistent set of notations, the density matrix in Eq. (9) of Sec. 1.1 of Ref. 15 is expressed as $\rho(\vec{r},\vec{r}\,')=2\sum_i\theta(\varepsilon_F-\varepsilon_i)\varphi_i^*(\vec{r}\,')\varphi_i(\vec{r})$. The carrier density of Ref. 15, $\rho(\vec{r})=\lim_{\vec{r}\,'\rightarrow\vec{r}}\rho(\vec{r},\vec{r}\,')$, is related to that of this work in Eq. (1) by $\rho(\vec{r})=\lim_{T\rightarrow 0}n(\vec{r})$. Therefore, the carrier density calculated in Ref. 15 is at zero temperature, whereas the carrier density presented in this work is a generalization of Ref. 15 to be at a finite temperature. Moreover, after some algebraic work, it can be shown that, as $T\rightarrow 0$ or $\beta\rightarrow\infty$, the carrier density expression in Eq. (6) reduces to the one-dimensional zero-temperature results given in Eqs. (16) and (17) of Sec. 1.4 of Ref. 15.

At the flat-band limit (∇V and $b\rightarrow 0$) or at the high-Fermi-level limit ($\varepsilon_F\gg V$), it follows immediately from Eq. (6) that

$$n(\vec{r})\rightarrow 2\left(\frac{m}{2\pi\hbar^2\beta}\right)^{d/2}\mathcal{F}_{d/2-1}[\beta(\varepsilon_F-V)],\tag{7}$$

which is indeed the carrier density of the homogeneous electron gas.[2,3]

III. RESULTS AND DISCUSSIONS

In contrast to the conventional HEG theory, the FOHEG theory of this work explicitly takes the first-order gradient of the electron potential energy into account. The DOS and the carrier density obtained by both methods will be compared in this section. For illustrative purposes, only three-dimensional ($d=3$) results are presented.

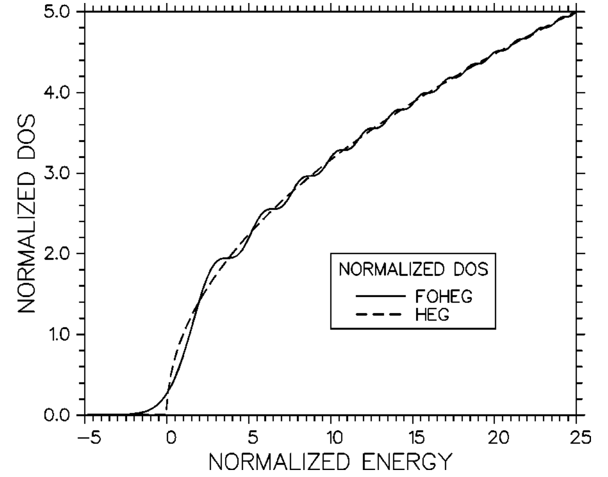

FIG. 1. The normalized density of states is plotted as a function of the normalized energy ($\bar{\varepsilon}=(\varepsilon-V)/b$). The DOS calculated by the FOHEG and HEG methods are sketched by solid and dashed lines, respectively.

The DOS obtained by the FOHEG method in Eq. (4) and by the HEG in Eq. (5) are plotted in Fig. 1 by solid and dashed lines, respectively. In this plot, the DOS is normalized by $(4/\sqrt{\pi})(m/2\pi\hbar^2)^{3/2}b^{1/2}$, and the normalized energy scale is $\bar{\varepsilon}=(\varepsilon-V)/b$ with $b^3=\hbar^2|\nabla V|^2/8m$. Comparison of the DOS calculated by the FOHEG and HEG methods shows two features. First, the potential gradient causes the waviness of the DOS curve. And the waviness gradually diminishes as the normalized energy increases, indicating that the effects of the potential gradient decrease with increasing energy. Similar results were reported in the high-field work of Ref. 5. Second, at an energy below the band edge ($\varepsilon<V$ or $\bar{\varepsilon}<0$), the HEG method predicts vanishing DOS, whereas the FOHEG shows that the potential gradient introduces states in the forbidden band gap of the flat-band theory. These induced states are due to quantum tunneling of wave functions beyond the classical turning point. The tunneling effectively lowers the band edge and consequently reduces the band gap, leading to a phenomenon called the tunneling-induced band-gap narrowing (TIBGN) in this work. Similar tunneling effects were reported in Ref. 14. The conventional HEG theory cannot account for this tunneling effect due to its negligence of the potential gradient.

In order to study the validity of the FOHEG and HEG methods, the carrier densities obtained by both approximations are computed and compared for systems with analytic solutions. The exact solution to an ideal spherical quantum dot with the confinement potential of $V(\vec{r})=\frac{1}{2}m\omega^2r^2$ is used as a test vehicle, where m, ω, and r are the effective mass, the angular frequency, and the radial distance from the origin, respectively.[10,11]

In this article, the ideal quantum dot is assumed to be manufactured by continually changing the composition x of $Al_xGa_{1-x}As$ crystal from 0 to 0.4 in the radial direction,

resulting in a parabolic confinement potential. If the compositional dependence of the effective mass of $Al_xGa_{1-x}As$ is ignored, the ideal quantum dot is essentially a three-dimensional simple harmonic oscillator with eigenenergy of $E_n = \hbar\omega(n+\frac{3}{2})$, where $n=0,1,2,\ldots$ and $n=0$ corresponds to the ground state.[4]

Since $Al_xGa_{1-x}As$ with $x \leq 0.4$ is a direct semiconductor and the conduction-band-edge difference between $Al_{0.4}Ga_{0.6}As$ and GaAs is about 324 meV,[26–28] the angular frequency of this ideal spherical quantum dot is taken so that $\hbar\omega = 30.3649$ meV to have enough quantum levels within the confinement potential. The temperature of 300 K and the GaAs effective mass of $m = 0.067 m_0$ is used in the computation, where m_0 is the electron rest mass.

The carrier densities obtained by the exact solution, the FOHEG, and the HEG approximations to the above hypothetic quantum dot are plotted in Fig. 2 by solid, dashed, and dotted lines, respectively, for Fermi energies at -100 meV, the zeroth ($E_0 = 45.548$ meV, ground level), the fourth ($E_4 = 167.01$ meV), and the eighth ($E_8 = 288.47$ meV) quantum levels of the quantum dot. Three features are observed in the figure. First, both the FOHEG and the HEG deviate from the exact solution at low Fermi energies (for instance, $\varepsilon_F = -100$ meV and E_0). There must be a large enough number of quantum levels below the Fermi level for the FOHEG prediction to sufficiently approach the exact solution (for instance, $\varepsilon_F = E_4$ and E_8). Second, the FOHEG results with successively higher Fermi levels ($\varepsilon_F = E_0, E_4$, and E_8) show that the approximation works better for systems with more quantum levels below the Fermi level. Third, at a radial location exceeding the classical turning point associated with the Fermi energy, $r_F = \sqrt{2\varepsilon_F/m\omega^2}$, the HEG starts to deviate from the exact solution more significantly, whereas the FOHEG better matches the exact results. This is because the tunneling of wave functions beyond the classical turning point is included in the theory of FOHEG as illustrated in Fig. 1.

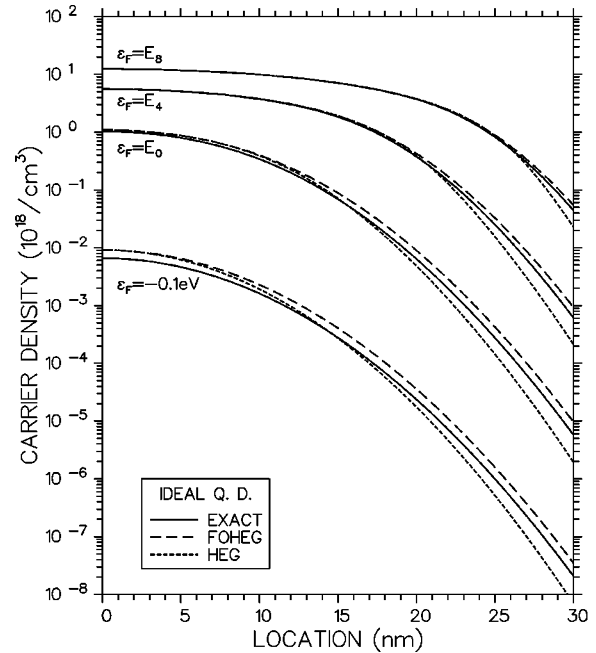

FIG. 2. The carrier densities of an ideal spherical quantum dot obtained by the exact solution, the FOHEG method, and the HEG method are plotted as functions of location by solid, dashed, and dotted lines, respectively, for Fermi energies at -100 meV, the zeroth ($E_0 = 45.548$ meV, ground level), the fourth ($E_4 = 167.01$ meV), and the eighth ($E_8 = 288.47$ meV) quantum levels of the ideal quantum dot.

IV. CONCLUSIONS

In this article, the conventional homogeneous electron gas theory is extended to explicitly include the effects of the first-order derivative of the potential energy, leading to an approximation called the first-order homogeneous electron gas theory by this work. The FOHEG theory is applicable to semiconductors with band bending at finite temperatures. The DOS and the carrier density are expressed by the analytic formulas given by Eqs. (4) and (6), respectively. Comparison with the exact solution to an ideal spherical quantum dot shows that the FOHEG calculation better matches the exact results than the HEG, especially at a location beyond the classical turning point.

ACKNOWLEDGMENTS

This research is supported by National Science Council, Taiwan, through Grant NSC90-2215-E-415-001.

[1] N. W. Ashcroft and N. D. Mermin, *Solid State Physics* (Saunders, Philadelphia, 1976).
[2] R.F. Pirret, *Semiconductor Device Fundamentals* (Addison-Wesley, Reading, 1996).
[3] S. M. Sze, *Physics of Semiconductor Devices*, 2nd ed. (Wiley, New York, 1981).
[4] J. J. Sakurai, *Modern Quantum Mechanics* (Benjamin/Cummings Menlo Park, CA, 1985).
[5] J.H. Davies and J.W. Wilkins, Phys. Rev. B **38**, 1667 (1988).
[6] W. Trzeciakowski and M. Gurioli, Phys. Rev. B **44**, 3880 (1991).
[7] W.L. Bloss, J. Appl. Phys. **66**, 1240 (1989).
[8] O.E. Raichev, P. Vasilopoulos, and F.T. Vasko, Phys. Rev. B **60**, 11 030 (1999).
[9] K. Chang and J.-B. Xia, J. Appl. Phys. **84**, 1454 (1998).
[10] C. Bose, J. Appl. Phys. **83**, 3089 (1998).
[11] G. Todorovic, V. Milanovic, Z. Ikonic, and D. Indjin, Phys. Rev. B **55**, 15 681 (1997).
[12] R. Buczko and F. Bassani, Phys. Rev. B **54**, 2667 (1996).
[13] A.H. Rodriguez, C. Trallero-Giner, S.E. Ulloa, and J. Marin-Antuna, Phys. Rev. B **63**, 125319 (2001).
[14] J.R. Lowney and H.S. Bennett, J. Appl. Phys. **65**, 4823 (1989).
[15] V.W. Macke and P. Rennert, Ann. Phys. (N.Y.) **12**, 84 (1963).

[16] V.W. Macke and P. Rennert, Ann. Phys. (N.Y.) **12**, 32 (1963).
[17] G. Paasch and H. Ubensee, Phys. Status Solidi B **113**, 165 (1982).
[18] G. Paasch and H. Ubensee, Phys. Status Solidi B **118**, 255 (1983).
[19] L.C.R. Alfred, Phys. Rev. **121**, 1275 (1961).
[20] L.C.R. Alfred, Phys. Rev. **125**, 214 (1962).
[21] T.L. Li, Chin. J. Phys. (Taipei) **39**, 453 (2001).
[22] F. Oberhettinger, *Tables of Fourier transforms and Fourier transforms of distributions* (Springer-Verlag, Berlin, 1990).
[23] H. Bateman, *Higher Transcendental Functions* (McGraw-Hill, New York, 1953), Vol. I, compiled by the staff of the Bateman Manuscript Project.
[24] *Handbook of Mathematical Functions with Formulas, Graphs, and Mathematical Tables*, edited by M. Abramowitz and I. E. Stegun, Nat. Bur. Stand. Appl. Math. Ser. No. 55 (U.S. GPO, Washington, D.C., 1972).
[25] M. Goano, Solid-State Electron. **36**, 217 (1993).
[26] N. Susa, IEEE J. Quantum Electron. **32**, 1760 (1996).
[27] Z.-Y. Deng, J.-K. Guo, and T.-R. Lai, Phys. Rev. B **50**, 5736 (1994).
[28] S. Adachi, J. Appl. Phys. **58**, R1 (1985).